Fourier Optics Based Analysis of Focal Plane Array of Distributed Absorbers

Shahab Oddin Dabironezare[1], Giorgio Carluccio[1], Angelo Freni[2], Andrea Neto[1], Nuria Llombart[1]
[1] Terahertz Sensing Group, Delft University of Technology, Delft, the Netherlands, dabironezare.shahab@ieee.org
[2] University of Florence, Florence, Italy

***Abstract* — Large format arrays of direct detectors are being used in the development of passive imaging cameras at sub-millimeter wavelengths. Several of these arrays are being developed with bare absorbing meshes without any antenna coupling (lens or horn) structures. The design of such arrays is typically done by resorting to geometrical considerations or basic broadside plane wave incidence analysis. This paper presents a spectral analysis technique of such focal plane arrays based on Fourier Optics. The analysis constitutes a step improvement with respect to previously used methods by providing an accurate and efficient way to estimate the point-source angular response and the throughput from a distributed incoherent source of an absorbing mesh in the focal plane of a quasi-optical component (e.g. a parabolic reflector or lens). The proposed technique is validated with full-wave simulations. Moreover, the paper compares the performance of arrays of bare absorbers in the focal plane of a quasi-optical component to those of corresponding antenna based arrays. It is found that absorbers lead to a comparable trade-off, in terms of spill-over and focusing efficiency, only for very tight samplings.**

***Index Terms*— Sub-mm absorbers, focal plane array, angular response, distributed source.**

I. Introduction

Future sub-millimeter imagers will require larger Field of Views (FoVs) with lower integration time to increase the image acquisition speed, for both security and space observation applications. The use of many detectors in the focal plane of an optical system (e.g., charged coupled device (CCD) like configuration) enables the use of systems with none or very limited mechanical scanning. As a consequence, the requirement of the detector's sensitivity is, in such configuration, relaxed thanks to the possibility of using an integration time comparable to the frame rate. In the last years, there has been a significant effort in developing large format Focal Plane Arrays (FPAs) of distributed absorbers based detectors with medium sensitivities for commercial sub-millimeter imaging cameras. Some current cameras make use of cryogenic Kinetic Inductance Detectors (KIDs) [1] or uncooled micro-bolometers [2].

The trade-offs which dominate the design of focal plane arrays based on antenna feeds are well-known, [3], [4], especially when the systems are required to operate over narrow frequency bands. Focal plane arrays of bare absorbers, however, are much less studied. The amount of power received and the obtainable angular resolution are significantly different from the one of antenna feeds. The difference raises from the fact that absorbers, unlike single port antennas, respond incoherently to multiple aperture field distributions induced by the incident field [4].

The paper is structured as follows. A tool based on a Fourier Optics (FO) spectral field representation coupled to a Floquet mode based circuit model is described in Sec. II. A schematic representation of the studied geometry is shown in Fig. 1. In Section III, the coupling of the absorber based imager to a point source is evaluated, and the system parameters such as the angular response, the aperture, and focusing efficiencies are described. In Section IV, the coupling of the imager to an incoherent distributed source is discussed, and the throughput of the system is derived in terms of the system parameters. The proposed method is validated with full wave simulations in Section V. Finally, Section VI contains some concluding remarks.

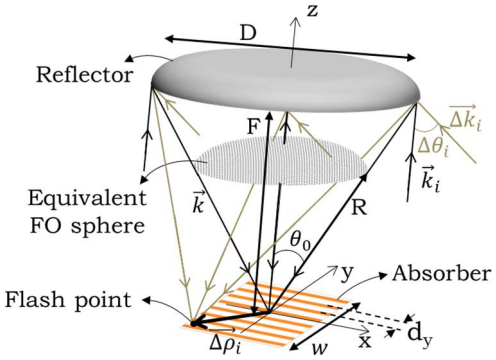

Fig. 1. The Fourier Optics scenario for broadside or oblique plane wave incidence onto a parabolic reflector with a square strip mesh absorber in its focal plane.

II. Fourier Optics Based Analysis

When an optical system is illuminated by a plane wave of amplitude, E_0, with wave-vector $\overline{\Delta\vec{k}_i} = k_0 \sin\Delta\theta_i \,(\cos\Delta\phi_i\,\hat{x} + \sin\Delta\phi_i\,\hat{y}) + k_0\cos\Delta\theta_i\,\hat{z}$ (Fig. 1) and polarization unit vector $\hat{p}_i$, an equivalent sphere centered at the focus of the focal plane can be used to evaluate a plane wave spectrum (PWS) representation of the *direct* focal field, $\vec{e}_d(\vec{\rho})$ [5]:

$$\vec{e}^{\,d}(\vec{\rho}) = \frac{1}{4\pi^2} \iint_{-\infty}^{+\infty} \vec{E}^{\,d}\left(\vec{k}_\rho\right) e^{-j\vec{k}_\rho\cdot\overline{\Delta\vec{\rho}_i}(1+\delta_i/F)} e^{j\vec{k}_\rho\cdot\vec{\rho}} k_\rho dk_\rho d\alpha \quad (1)$$

where $\vec{E}^d(\vec{k}_\rho) = j2\pi R e^{-jkR}\vec{E}^{GO}(\vec{k}_\rho, \overrightarrow{\Delta k}_{\rho i}=0)/\sqrt{k^2-k_\rho^2}$ with R being the radius of the equivalent sphere (Fig. 1), $\overrightarrow{\Delta k}_{\rho i}$ is the ρ-component of the incident wave vector, $\vec{k}_\rho$ the spectral vector given by $\vec{k}_\rho = k_0 \sin\theta\,(\cos\phi\,\hat{x} + \sin\phi\,\hat{y})$, $\overrightarrow{\Delta\rho}_i = F\overrightarrow{\Delta k}_{\rho i}/k_0$ is the flash point position, $e^{-j\overrightarrow{\Delta\rho}_i\cdot\vec{k}_\rho(1+\delta_i(\theta)/F)}$ corresponds to the linear and comma phase terms, and $\delta_i(\theta) = 2F/(1+\cos\theta) - F$ indicates the distance between the reflector surface and the equivalent sphere. $\vec{E}^{GO}(\vec{k}_\rho, \overrightarrow{\Delta k}_{\rho i}=0)$ is the Geometrical Optics (GO) field component tangent to the equivalent sphere. This GO field is only defined over the angular sector subtended by the optical system ($\theta < \theta_0$), as shown in Fig. 1. The analytical expression of this field, and its limits of applicability, are given in [6] for a parabolic reflector with a focal distance, $F = R$, as:

$$\vec{E}^{GO}(\vec{k}_\rho, \overrightarrow{\Delta k}_{\rho i}=0) = \frac{j2k_0E_0}{k_0+k_z}e^{-j\Delta k_{zi}F}\left[\hat{\theta}(\hat{p}_i\cdot\hat{k}_\rho) + \hat{\phi}(\hat{p}_i\cdot\hat{\alpha})\right]\mathrm{circ}(k_\rho, k_{\rho 0}) \quad (2)$$

where $\hat{\alpha} = (-k_y\hat{x} + k_x\hat{y})/k_\rho$, and Δk_{zi} are the ρ- and z-components of the incident wave vector, respectively, and $k_{\rho 0} = k_0\sin\theta_0$, with θ_0 being the reflector subtended angle.

The coupling mechanism between the impinging field and the absorber can be represented via an equivalent Floquet circuit, as described in [5]. The periodic absorbing mesh response to a plane wave is included in the circuit via an equivalent admittance matrix, $\bar{Y}_{abs}(\vec{k}_\rho)$. The components of this matrix can be derived analytically for a few structures or evaluated numerically using periodic boundary conditions via a commercial electromagnetic tool.

By solving the equivalent circuit, one can evaluate the spectral total average fields, $[\vec{E}^t, \vec{H}^t]$, at any z-quote, that includes both the absorber and optical system spectral responses. The spatial fields representing the response of the absorber to the optical system under a slightly off broadside incidence, $\vec{e}^t(\vec{\rho}, \overrightarrow{\Delta k}_{\rho i})$, can therefore be evaluated as the inverse Fourier transform of the spectral total field evaluated at broadside times the linear and coma phase terms, i.e.,

$$\vec{e}^t(\vec{\rho}, z, \overrightarrow{\Delta k}_{\rho i}) = \frac{1}{4\pi^2}\iint_{-\infty}^{+\infty}\vec{E}^t(\vec{k}_\rho, z, \overrightarrow{\Delta k}_{\rho i}=0)e^{-j\vec{k}_\rho\cdot\overrightarrow{\Delta\rho}_i(1+\delta_i/F)}e^{j\vec{k}_\rho\cdot\vec{\rho}}k_\rho dk_\rho d\alpha \quad (3)$$

III. Point-Source Response

In this section, we derive the response of resistive periodic absorber under a focusing system when the latter is illuminated by a single plane wave of amplitude E_0, impinging from a direction $\overrightarrow{\Delta k}_i$ (Fig. 1). Using (3), we can estimate the total spatial electric and magnetic field, $\vec{e}^t(\vec{\rho})$ and $\vec{h}^t(\vec{\rho})$, at the focal plane. Once that the fields are known, the power absorbed by a finite periodic mesh can be evaluated, assuming local periodicity, as the integral, over the absorber area w, of the z-component of the Poynting's vector associated to the spatial total fields as follows:

$$P_{abs}(f, \overrightarrow{\Delta k}_{\rho i}) = \frac{1}{2}Re\left\{\iint_{-w/2}^{w/2}\left[\vec{e}_t(\vec{\rho}, \overrightarrow{\Delta k}_{\rho i})\times\vec{h}_t^*(\vec{\rho}, \overrightarrow{\Delta k}_{\rho i})\right]\cdot\hat{z}\,d\vec{\rho}\right\} \quad (4)$$

The aperture efficiency, η_{ap}, of an absorber under a reflector relates the effective area, A_{eff}, to the physical area, A_{ref}, of the reflector. This efficiency, can be calculated as the ratio between the power absorbed, (4), for broadside incidence, and the power incident to the reflector, $P_{in} = 0.5|E_0|^2 A_{ref}/\zeta_0$, as:

$$\eta_{ap}(f) = P_{abs}(f, \overrightarrow{\Delta k}_{\rho i}=0)/P_{in} \quad (5)$$

The angular response of an absorber coupled to an optical system, can be evaluated by calculating how much the absorbed power (4) changes versus the impinging plane wave wave-vector $\overrightarrow{\Delta k}_{\rho i}$. A normalized angular response will be defined here as follows:

$$F(f, \Delta\theta_i, \Delta\phi_i) = P_{abs}(f, \overrightarrow{\Delta k}_{\rho i})/P_{abs}(f, 0) \quad (6)$$

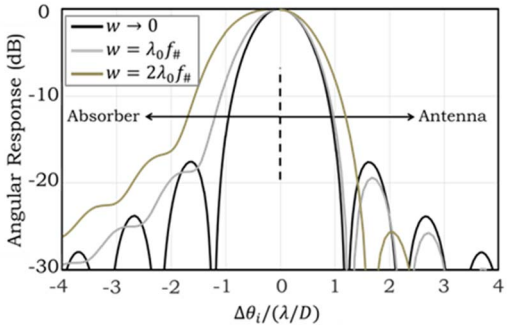

Fig. 2. Angular response to a plane wave impinging from $\Delta\theta_i$ of both an ideal absorber, and an uniform aperture antenna coupled to a parabolic reflector with $f_\# = 2$.

Figure 2 shows the angular response of the ideal absorber (a thin continuous conductive sheet with a surface resistance of $R_s = \zeta_0 = 377\Omega/\square$ on top of quarter wavelength backshort, $h_{bs} = \lambda/4$) and a uniform antenna (an impedance matched antenna with uniform square electric distribution above an infinite ground plane) coupled to a parabolic reflector with $f_\# = 2$ for different feed sizes. It can be noted that, for both cases, the angular response is the well-known Airy distribution for physical dimensions small in terms of $\lambda f_\#$. Instead the imager angular response gets much wider when the physical dimension of the absorber increases than in the case of antennas. This implies that, as the absorber

size increases, the HPBW increases faster than for a uniform current antenna.

In Fig. 2, we have shown that the angular resolution of the imager of Fig. 1 gets reduced with the dimension of the absorber. To quantify this angular resolution penalty, we now introduce a *focusing efficiency* that relates the solid angle of the Airy pattern, Ω_{Airy} to that of the actual imager angular response, Ω_o, as follows:

$$\eta_f = \frac{\Omega_{Airy}}{\Omega_o} \tag{7}$$

where the solid angle of the Airy pattern and the imager are $\Omega_{Airy} = \lambda^2/A_{ref}$, and $\Omega_o = \int_0^{2\pi}\int_0^{\frac{\pi}{2}} F(f,\theta,\phi) sin\theta d\theta d\phi$, respectively.

The focusing efficiency quantifies how much the angular response enlarges with respect to the diffraction limited case. In case of antenna feeds, this efficiency corresponds to the ratio between the achieved directivity in the optical system and the directivity of a uniform circular aperture. In Fig. 3, this efficiency is shown as a function of the feed size normalized to $\lambda f_\#$ together with the spill-over efficiency for the case of an ideal absorber or a uniform antenna under a reflector of $f_\# = 2$.

The spill-over efficiencies (for the antenna calculated as defined in [7]) are nearly the same for both types of feeds, but the focusing efficiency is significantly different. Indeed, except for very small sizes, the antenna type feeds are more directive with respect to a commensurate absorber.

To quantify the trade-off between the two different efficiencies in Fig. 3, we also plot the product of these two efficiencies. Note that, in the case of antennas the product of the spill over and focusing efficiencies corresponds to the aperture efficiency [7], except for any other losses in the antenna feed itself. Instead, in the case of absorbers this product is simply a figure of merit that reminds the designer that larger absorbers lead to an inefficient use of the reflector aperture from an angular resolving point of view. As it can be seen from Fig. 3, bare absorber FPAs with $w \leq 0.75\lambda f_\#$ have focusing efficiencies higher than 80%, and therefore the product of their two efficiencies are comparable to those of antenna feeds.

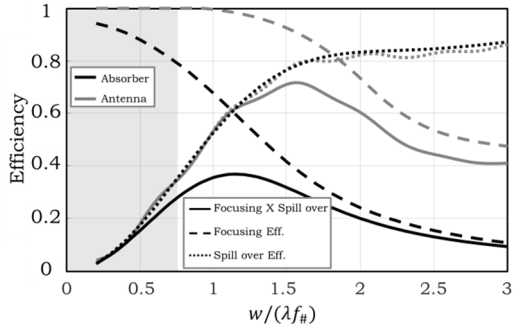

Fig. 3. Focusing and spill-over efficiencies for both ideal antenna and absorbers, with a square dimension of side length w, under a reflector with $f_\# = 2$. The grey area indicates the region where the product of the two efficiencies, for the absorber and antenna feeds, are comparable.

IV. DISTRIBUTED-SOURCE RESPONSE

The sensitivity of a passive imager can be related to the ability of the system in detecting variations in the temperature of a distributed incoherent source, [8], [9]. Thus, it is related to the power received from a distributed source. This power, P_{abs}^{DS}, over a certain narrow bandwidth BW, from incoherent sources operating in Rayleigh Jean's limit with an average temperature T_s, and distributed over the full solid angle, can be expressed as [5]:

$$P_{abs}^{DS} \approx k_B T_s BW \frac{\eta_{ap}(f_0)}{\eta_f(f_0)} \tag{8}$$

where k_B is the Boltzmann's constant. In the scientific literature, instead of the ratio $\eta_{ap}(f_0)/\eta_f(f_0)$ one typically finds the normalized throughput, $A_{ref}\Omega_o/\lambda_0^2$, or number of effective modes of the system [9], [10].

Since for single-mode antennas the aperture efficiency is proportional to the focusing efficiency itself, $\eta_{ap}^{ant} = \eta_{rad}\eta_f$, where η_{rad} is the radiation efficiency, the normalized throughput becomes $\left(A_{ref}\Omega_A/\lambda_0^2\right)^{ant} = \eta_{rad}(f_0) \leq 1$. Whereas for bare absorber, $A_{ref}\Omega_A/\lambda_0^2$ can be a much larger number.

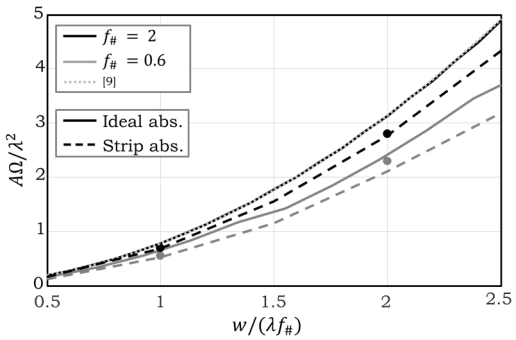

Fig. 4. Normalized throughput calculated as η_{ap}/η_f versus the absorber size, w, for two optical systems with $f_\# = 0.6$ (grey) and $f_\# = 2$ (black). The solid lines are related to the ideal absorbers, the dashed lines to an absorber based on resistive strips, and the dots to the relevant performed full wave simulations.

The term $\eta_{ap}(f_0)/\eta_f(f_0)$ is plotted in Fig. 4 for the case of an ideal absorber under a parabolic reflector with $f_\# = 2$. The normalized throughput $A_{ref}\Omega_o/\lambda_0^2$, derived accordingly to [9] by using Airy Pattern considerations, is superimposed to the curve shown in Fig. 4. The agreement is very good since the calculations were done for an ideal absorber under a large $f_\#$ parabolic reflector. However, the analysis proposed in this paper can accurately quantify the normalized throughput for many other cases. As an example, Fig. 4 also shows the normalized throughput for an ideal absorber under a $f_\# = 0.6$ parabolic reflector. In such case, its value differs significantly from the one calculated in [9], leading to a lower received power from a distributed incoherent source and, therefore, degradation of sensitivity.

V. NUMERICAL EXAMPLES

In this section, the results calculated with the proposed methodology are compared with those obtained by using full wave simulations (as described in [5]). An absorber made of linear resistive strips above a $\lambda/4$ backing reflector is considered as a test case. The absorber is composed of resistive mesh strips with a surface resistance of $R_s = 10\ \Omega/\square$ and width of 2.7 μm. The strips have a periodicity of $d_y = 102$ μm, and back short distance of $h_{bs} = 150$ μm. The total dimension of the absorber is $w \times w$ (Fig. 1). The operating frequency for this example is 500 GHz. The parabolic reflector has a diameter of $D = 100\lambda$, and the incident plane wave is assumed having amplitude $|E_0| = 1\ \mathrm{V/m}$ and polarization along x.

In Figs. 5(a) and (b) the power absorbed by the linear strip mesh, placed under a parabolic reflector with $f_\# = 2$, is shown versus the plane wave angle of incidence, for two different physical dimensions of the absorber. The agreement between both methods is excellent.

In Figs. 5(c) and (d) the same scenario is performed for absorbers under a parabolic reflector with $f_\# = 0.6$. The lower is the $f_\#$, the more difficult it is to evaluate the performances of absorbers under optical systems. Firstly, the direct field changes significantly even for an incident angle of a couple of HPBWs due to the coma phase term. Secondly, the absorber plane wave response can affect significantly the shape of the total spatial fields. Thirdly, the absorber's overall physical dimension can be comparable to the wavelength, or even smaller, making the FO + Floquet mode approach not applicable. Despite the mentioned difficulties, the agreement is still quite good even if the absorber is small in terms of the wavelength. Moreover, for both cases, $f_\# = 2$ and 0.6, the normalized throughput, the aperture, and focusing efficiencies are also calculated, with excellent agreement to the full wave simulations. In Fig. 4, the corresponding throughputs are also shown for the theoretical method and full wave simulations.

VI. CONCLUSION

Passive imaging cameras at sub-millimeter wavelengths are being developed using bare absorbing meshes without any antenna coupling (lens or horn) structures in the focal plane of a focusing system. The design of such arrays is typically done resorting to geometrical considerations or basic broadside plane wave incidence analysis. This work presents a spectral electromagnetic model that is based on linking a Plane Wave Spectral representation of the direct field focused by the optical system with a Floquet Wave representation of the field in the absorbing mesh. The results obtained with the present model have been compared, with excellent agreement, with those obtained with full wave simulations. Thus, the proposed spectral method provides an accurate and efficient way to estimate the key optical properties of the imager inside the region of validity of the Fourier Optics. In particular, it has been found that the use of bare absorber FPAs leads to a reduced focusing efficiency of the main optical aperture with respect to antenna feeds.

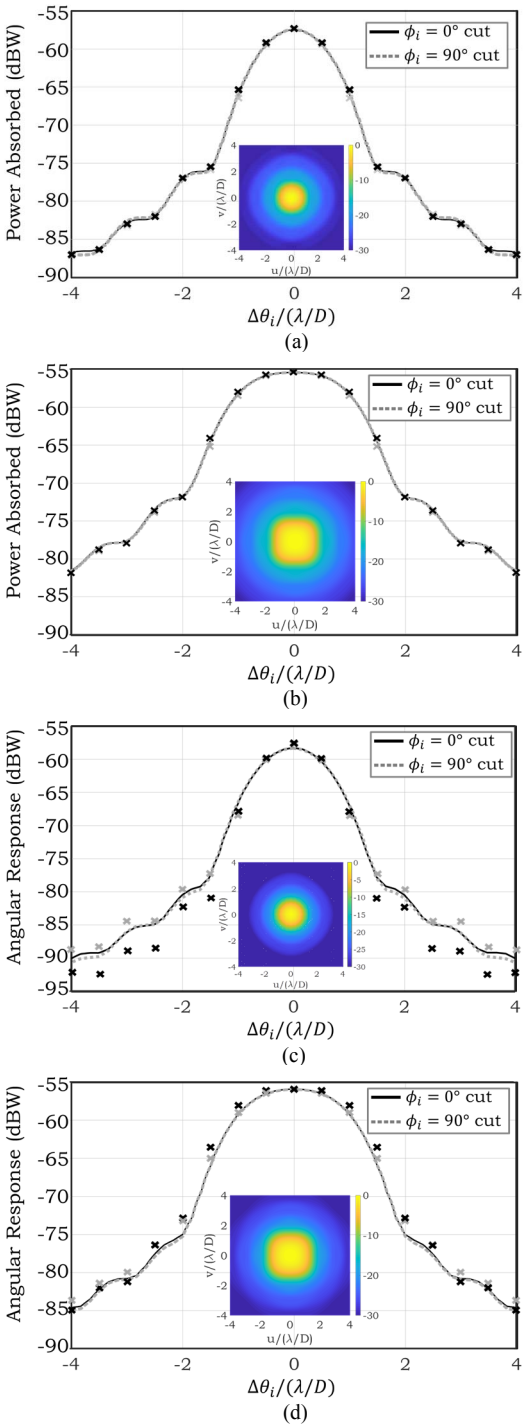

Fig. 5. Power absorbed versus the plane wave incident angle of a linear strip absorber with side length w coupled to a reflector when (a) $f_\# = 2$ and $w = 1\lambda f_\#$. (b) $f_\# = 2$ and $w = 2\lambda f_\#$. (c) $f_\# = 0.6$ and $w = 1\lambda f_\#$. (d) $f_\# = 0.6$ and $w = 2\lambda f_\#$. Solid lines: calculated by using the proposed method. Cross marks: obtained via full wave simulations.

Only very tightly sampled absorber based FPAs lead to a comparable trade-offs in terms of received power and angular resolution, when compared to antenna based FPAs.

For antennas it is well known that a distributed incoherent source is $P_{ant}^{DS} = \eta_{rad} k_b T_s BW$, and for absorber FPAs, the corresponding received power is typically quantified by introducing an effective number of modes: $P_{abs}^{DS} = m_{eff} \times k_b T_s BW$. Here it is shown that m_{eff} is conveniently evaluated as the ratio between the aperture, η_{ap} and the focusing efficiencies, η_f, which required the characterization of the focusing system in reception to be introduced.

ACKNOWLEDGMENT

This work was supported by ERC Starting Grant (ERC-2014-StG LAA-THz-CC), No. 639749.

REFERENCES

[1] A. Timofeev, J. Luomahaara, L. Grönberg, A. Mäyrä, H. Sipola, M. Aikio, M. Metso, V. Vesterinen, K. Tappura, J. Ala-Laurinaho, A. Luukanen, and J. Hassel, "Optical and electrical characterization of a large kinetic inductance bolometer focal plane array," *IEEE Trans. Terahertz Sci. Technol.*, vol. 7, no. 2, pp. 218–224, Mar. 2017.

[2] N. Oda, S. Kurashina, M. Miyoshi, K. Doi, T. Ishi, T. Sudou, T. Morimoto, H. Goto, T. Sasaki, "Microbolometer Terahertz focal plane array and camera with improved sensitivity in the sub-Terahertz region," *J. Infrared Milli. Terahz Waves*, vol. 36, no. 10, pp. 947–960, Oct. 2015.

[3] J. F. Johansson, "Millimeter-wave imaging theory and experiments," *Onsala Space Observatory Research Report*, No. 151, vol. 1, p. 1, 1986.

[4] S. Rao, L. Shafai, and S. K. Sharma, Ed., *Handbook of Reflector Antennas and Feed Systems Volume II*, Artech House, 2013.

[5] N. Llombart, S.O. Dabironezare, G. Carluccio, A. Freni, and A. Neto, "Fourier optics analysis of focal plane arrays of distributed absorbers: skew incidence," *IEEE Trans. Antennas Propag.*, submitted.

[6] N. Llombart, B. Blázquez, A. Freni, and A. Neto, "Fourier optics for the analysis of distributed absorbers under THz focusing systems," *IEEE Trans. Terahertz Sci. Technol.*, vol. 5, no. 4, pp. 573–583, July 2015.

[7] J. D. Kraus, *Antennas for all applications*, second edition, Tata McGraw-Hill, p. 575, 1997.

[8] S. L. van Berkel, O. Yurduseven, A. Freni, A. Neto, and N. Llombart, "THz imaging using uncooled wideband direct detection focal plane arrays," *IEEE Trans. Terahertz Sci. Technol.*, vol. 7, no. 5, pp. 481–492, Sept. 2017.

[9] M. J. Griffin, J. J. Bock, and W. K. Gear, "Relative performance of filled and feedhorn-coupled focal-plane architectures," *Appl. Optics*, vol. 41, no. 31, pp. 6543–6554, Nov. 2002.

[10] D. Rutledge and S. Schwarz, "Planar multimode detector arrays for infrared and millimeter-wave applications," *IEEE J. Quantum Electron.*, vol. 17, no. 3, pp. 407–414, Mar. 1981.